Estimation of the mode conversion effect on the determination of southern boundary for the ~ 100 MeV electron precipitations

G. F. Remenets [1], A. M. Astafiev [1]

[1]Department of Physics, Saint Petersburg State University, Saint Petersburg, 199034, Russian Federation

Key Points:

- The influence of the ultraenergetic relativistic electron precipitations on mode conversion in the terrestrial waveguide was analyzed.
- New statement of a mode conversion problem was used.
- The effect of a normal wave conversion may be neglected in the problem of southern boundary determination if the precipitations are not powerful.

Corresponding author: George Remenets, `g.remenets@spbu.ru`

Abstract

The parameters of sporadic D_s layer of electric conductivity caused by ultraenergetic relativistic electron (URE) precipitations are determined due to indirect electromagnetic method. Previously we determined the southern boundaries of these precipitations in the frames of the following supposition: the effect of a normal wave reflection and its conversion into other normal waves on the boundary between disturbed and undisturbed parts of a radio path might have been ignored. Now we show by accurate simulation that it was true for strong and moderate disturbances. For the powerful URE disturbances the effect is significant. In order to obtain this result we had to change a traditional problem statement about a normal wave conversion in the terrestrial waveguide and to solve numerically this new problem with a ″volume″ inhomogeneity.

1 Introduction

A phenomenon of ultraenergetic relativistic electron (URE) precipitation with abnormally high intensity into polar atmosphere was stated by the help of indirect very low frequency (VLF)-method (*Remenets and Beloglazov*(1985), Remenets and Beloglazov(1985); *Remenets and Beloglazov*(2013), Remenets and Beloglazov(2013)) more than 30 years ago. During these years the monitoring of the fluxes of $\sim$ 100 MeV electrons in the near cosmos did not appear although the fluxes of highly-energetic relativistic electrons (HRE) with energy from $\sim$ 1 to $\sim$ 10 MeV were measured about the same 30 years (*Callis et al.*(1991), Callis et al.(1991); *Pesnell et al.*(1999), Pesnell et al.(1999)) and the fluxes of GeV electrons were monitored more than 10 years (*Andriani et al.*(2017), Andriani et al.(2017)). The window (gap) between these measurements was partially overlapped by the ground VLF measurements, which we have indicated above.

The VLF waves generated by a ground based transmitter and propagating in a terrestrial waveguide between two conducting mediums (which are the ground and bottom ionosphere) are sensitive to the time dependence of electric conductivity of this bottom and to its dynamics being caused either due to the ionization of neutrals by the precipitating electrons or by hard electromagnetic radiation. At the same time the ultraenergetic relativistic electrons (URE′s) are the sources of very significant bremsstrahlung radiation in the atmosphere (*Satio Hayakawa*(1969), Satio Hayakawa(1969); *Remenets and Beloglazov*(2013), Remenets and Beloglazov(2013)) if the density of corpuscular flux is abnormally high (*Remenets and Beloglazov*(2013), Remenets and Beloglazov(2013)).

It is known that the electrons with energy $\sim$ 100 MeV do not penetrate mainly into the atmosphere deeper than the altitude with the pressure $50g/cm^2$, that is, deeper $\sim$ 40 km. Therefore, significant electric conductivity, registered by VLF-method at the altitudes 30 km and lower (*Beloglazov and Remenets*(2005), Beloglazov and Remenets(2005)) can be caused only by the bremsstrahlung X- and gamma rays. These rays created a sporadic D_s - layer, which manifesed itself in both existing numerical solutions of the inverse VLF problem (*Remenets*(1997), Remenets(1997); *Beloglazov and Remenets*(2005), Beloglazov and Remenets(2005); *Remenets and Beloglazov*(2013), Remenets and Beloglazov(2013)). The pointed solutions were based on a theory of VLF wave propagation in near-Earth wave guide, that is, they were based on the Maxwell′s equation consequences for a physics model of waveguide (?, ?; *Makarov et al.*(1993), Makarov et al.(1993)). One of the pointed solutions of the inverse problem uses the ray (″hop″) theory (using the Watson-Fock diffraction wave and two rays reflecting from a ″bottom″ of atmosphere ionized) (*Remenets*(1997), Remenets(1997); *Bondarenko and Remenets*(2001), Bondarenko and Remenets(2001); *Remenets and Beloglazov*(2013), Remenets and Beloglazov(2013); *Remenets and Astafiev*(2015), Remenets and Astafiev(2015); *Remenets and Astafiev*(2016), Remenets and Astafiev(2016)), and the other version of invers problem uses the normal waves (modes) in the waveguide (*Remenets*(1994), Remenets(1994); *Remenets*(1997), Remenets(1997); *Beloglazov et al.*(1998), Beloglazov et al.(1998); *Beloglazov and Remenets*(2005), Beloglazov and Remenets(2005)). Both types of solutions complement each other and give practically the same values of effective heights (*Remenets*(1997), Remenets(1997); *Beloglazov and Remenets*(2005), Beloglazov and Remenets(2005)).

In order to model the D_s-layer conductivity as function of altitude z we used in the last pointed works an approximation of its profile with two free parameters – the thickness $z_1 \div z_0$ of its homogeneous conductivity and the gradient β of its exponential dependence at altitudes below z_1, Figure 1. The upper part of ionosphere higher than $z_0 \sim$ 60 km was considered undisturbed by the URE precipitations, and was approximated by exponential dependence on z for an electron concentration profile $N_e(z)$ (*Beloglazov and Zabavina*(1982a), Beloglazov and Zabavina(1982a); *Beloglazov and Zabavina*(1982b), Beloglazov and Zabavina(1982b)). The logarithm of schematic σ function (a dotted curve with number 4 for Figure 1.) has two $''$elbows$''$ at altitudes z_0 and z_1. With such type of approximation for a sporadic D_s-layer the inverse problems were solved. The output parameters of the solution were the z_1 and β, and their values are represented for several time moments of the URE precipitations on 29 September 1989, 21 and 22 January 2002, the Table 1 and Table 2, which are reproduced from the works (*Remenets*(1997), Remenets(1997); *Beloglazov and Remenets*(2005), Beloglazov and Remenets(2005)).

The approximation parameters, z_1 and β for profile $N_e(z)$ (with the profile of effective electron collisions having been fixed), were found due to the procedure of minimization of a discrepancy-function for 3 frequencies between the experimental and calculated amplitude and phase variations of signals caused by an URE precipitation. It is necessary to note that when one tries to satisfy the experimental VLF data (amplitude and phase variations for 3 frequencies) for the auroral radio path S_1 (Aldra-Apatity) with length $\sim$ 900 km (in the cases of UREP disturbances) with the help of *monotonous* exponential electron concentration profile $N_e(z)$ it turns out that it is impossible to do it correctly (reliably): the amplitude data demand for themselves an $N_e(z)$ with its effective height at 20 km lower than the effective height of an electron concentration profile suitable for the phase data. It was possible to overpass this contradiction only by an adoption that for satisfying the amplitude and phase data simultaneously it was necessary to use not monotonic *effective* profile N_e, the corresponding profile of electric conductivity having been monotonic. This qualitative discrepancy between the $\sigma(z)$ and $N_e(z)$ profiles is caused by the item that electric conductivity below 50 km is determined by the electrons and ions, so $N_e(z)$ is a profile of the **effective electron concentration**.

Now we return to the Table 1 and Table 2 for which a comparison of experimental and theoretical magnitude values is represented. The profile of electron collision frequency (with the atoms of air) was accepted for these calculations as it follows: $\nu_{eff} = 0.87\ 10^7 \exp b(z - 70km)$ 1/s with $b = -0.14$ 1/km . Theoretical values of field magnitudes (the digits in the brackets) were calculated using the values z_1 and β for the σ-profile with the number 4 kind, Figure 1. The description of the table parameters and magnitudes is the following:

an index $j = 1, 2, 3$ is the number of frequency used in the experiment (10.2, 12.1, 13.6 kHz correspondingly);

$(A_j)_c$ – a value of amplitude in undisturbed (calm) conditions; $(A_j)_d$ – a value of disturbed amplitude at UT moment pointed in first lines of the Tables 1 and 2;

$(\varphi_j)_c$ – a value of phase in undisturbed conditions; $(\varphi_j)_d$ – a value of disturbed phase at UT moment pointed in first line.

The pointed magnitudes (without brackets) are the input ones for an inverse problem. The other parameters of the tables below the amplitude and phase data are the output magnitudes:

z_1 and β; h' – an effective height of a waveguide with a nonmonotonic $N_e(z)$ profile, acquired by using the amplitude and phase data (6 magnitudes); h'' – an effective height of a waveguide with a nonmonotonic $N_e(z)$-profile, gotten by using phase data (3 magnitudes); h''' – an effective height of a waveguide with a nonmonotonic $N_e(z)$-profile, gotten by using phase data (3 magnitudes); h – an effective height of a waveguide, gotten for the same time moments by another VLF inverse problem solution (*Remenets and Beloglazov*(1985), Remenets and Beloglazov(1985); *Remenets and Beloglazov*(1992), Remenets and Beloglazov(1992)); this method is a self-consistent one, that is, it does not need the input geophysical data, and is based on the experimental VLF data and the theory of wave propagation completely.

Concluding the discussion of the Table 1 and Table 2 we ought to point out that the effective heights with primes for a given $N_e(z)$-profile were calculated by a special procedure (*Galyuk and Ivanov* (1978), Galyuk and Ivanov (1978); *Remenets and Beloglazov*(2013), Remenets and Beloglazov(2013); *Remenets and Astafiev*(2019), Remenets and Astafiev(2019)): 1-st step – the value of an impedance function is calculated for any altitude at which the electric conductivity is negligible by integration of not linear equation for impedance function from z_2 top to down; 2-d step – the gotten value is used as the initial value for integration of the impedance function equation for empty medium in opposite direction until a height h' for which the impedance function becomes real (*Galyuk and Ivanov* (1978), Galyuk and Ivanov (1978)). Such acquired height is called an effective one due to the statement that the phase path of a propagating mode in the real terrestrial waveguide is the same as in a model air waveguide with h' height. Therefore, the tables represented and described is a part of electromagnetic proof of sporadic D_s-layer existence. Now we pass to new calculation problem.

According to the z_1 values of Table 1 (which is for daytime conditions) it can be seen that these values differ negligibly from z_0. Therefore, we use below an approximation with one parameter – gradient β, and $z_1 \equiv z_0$ being adopted (*Bondarenko and Remenets*(2001), Bondarenko and Remenets(2001)). Therefore, we use at present publication one ″elbow″ approximation of the D_s-layer, the curves 1 – 3 for Figure 1.

2 Physical and mathematical problems

In our works (*Remenets and Astafiev*(2015), Remenets and Astafiev(2015); *Remenets and Astafiev*(2016), Remenets and Astafiev(2016)) we have determined the southern boundaries of URE precipitations which had been registered (about 300 events during 1982 – 1992 years) by a VLF-method. The method was based on continuous ground-based measurements (by the scientists of the Polar Geophysical Institute – RAS, Apatity, Murmansk reg., Russia) of amplitude and phase disturbances for several VLF-signals for two radio paths: one path S_1 was completely auroral and the second path S_2 (United Kingdom – Kola Peninsula) was partly auroral. The part of the atmosphere which is higher than 61° of magnetic latitude is electrically disturbed during an URE precipitation (UREP). This boundary is higher at several degrees than the analog boundary for the protons with energy 0.1 – 0.4 GeV, figure 39 of the work (*Andriani et al.*(2017), Andriani et al.(2017)). Due to an URE precipitation the profile of electric conductivity is changing below a certain altitude (z_0), under a regular ionosphere D-layer a sporadic D_s-layer appears caused by the bremsstrahlung X-ray radiation which is generated by the precipitating electrons. Therefore, the radio path S_2 becomes significantly inhomogeneous along its length. The breaking of radio path homogeneity we model by an abrupt hop of electric properties at a distance D from a receiver, and the properties for both sides from this boundary are being homogeneous along the path but different. The pointed inhomogeneity of radio path is the cause of conversion of a normal wave of terrestrial wave guide at other normal waves. Having a certain quantitative estimations about a significance of this effect on the base of our predecessor calculations for other types of inhomogeneity (such as an abrupt change of electric properties of ground, an abrupt change of waveguide effective height) (*Bahar and Wait*(1965), Bahar and Wait(1965); *Wait*(1968), Wait(1968); *Wait and Spies*(1968), Wait and Spies(1968); *Pappert and Morfitt*(1972), Pappert and Morfitt(1972); *Smith*(1977), Smith(1977); *Osadchiy and Remenets*(1979), Osadchiy and Remenets(1979); *Pappert and Ferguson*(1986), Pappert and Ferguson(1986)) we ignored the pointed effect in the publications (*Remenets and Astafiev*(2015), Remenets and Astafiev(2015); *Remenets and Astafiev*(2016), Remenets and Astafiev(2016)). Nevertheless, here we have to justify our previous neglect by taking into account the effect of conversion of a normal wave in other ones and to point for what type of UREP (moderate, strong or powerful) it is necessary to take into account this effect while a boundary latitude calculation. For this purpose we would to change the traditional problem statement.

Let us give short comments of the works devoted to the mode conversion in a terrestrial waveguide taking into account that the anisotropic properties of low ionosphere are absolutely negligible for us due to the analysis here only the daytime disturbances. For them the effective height h of a waveguide is falling down from 60 to 50, 40 and even 30 km during the UREPs. One ought to take into account that this height is always present inside the altitude part of ionosphere which determines a mode reflection to ground. Among the works of pointed type *Bahar and Wait*(1965) (Bahar and Wait(1965)); *Wait*(1968) (Wait(1968)); *Wait and Spies*(1968) (Wait and Spies(1968)) there are the following ones: a work, in which an abrupt change of top waveguide boundary with given impedance is introduced, the works with the models of the day-night transition in a VLF waveguide, and cylindrical model of the wave guide instead of spherical one being used. This type of model does not suit us because of the following issues:

1) the eigenfunctions of day-side do not orthogonal in the night-side section and vice versa due to the different widths of the left and right sections, therefore this item generates an uncontrolled error;

2) the named eigenfunctions are accurately orthogonal only if the impedance of a waveguide top boundary is constant, that is, the impedance does not depend on the eigenvalue. But the last item works sufficiently good only at high altitudes where the electric conductivity is sufficiently high, and this item works badly if the bottom boundary is chosen for an altitude where the electric conductivity is low.

3) In the works (*Pappert and Morfitt*(1972), Pappert and Morfitt(1972); *Pappert and Ferguson*(1986), Pappert and Ferguson(1986)) the plain waveguide model was used. This type of modeling does not suit us too, because the height gain functions for a plain waveguide and a spherical waveguide are significantly different for relatively high frequencies.

4) In the work (*Galejs*(1964), Galejs(1964)) the author used the plain model too taking into account the sphericity effect either by a certain approximation or using a cylindrical waveguide (*Galejs*(1968), Galejs(1968); *Galejs*(1969), Galejs(1969)) according to J. R. Wait (*Wait*(1964), Wait(1964)).

The pointed mathematical differences are relatively subtle notions, but it is necessary to pay main attention that in all mentioned works the heterogeneities were lateral (sidelong) ones: either an abrupt change of the boundary surface impedance or a change of the height of an empty waveguide (modeling of a transition from day to night) . Therefore, it is necessary *in our case* to make another statement of problem about the normal waves conversion *on an abrupt radial change of the medium properties* without artificial and weakly controlled dividing the transverse conducting medium at two following parts: the bottom part which is empty medium (vacuum) and the top conducting part which is not involved in the mode conversion calculations directly.

In our case the middle altitudes of the waveguide atmosphere are disturbed due to an appearance of a D_s-layer. Therefore, we work with a transverse radial inhomogeneity which is homogeneous along a disturbed part of the radio path. The problem with such $''$volume$''$ inhomogeneity will be solved in this paper. To-day, when the simulation possibilities are much greater than 50 –60 years ago it is not necessary to pass from spherical geometry to the cylindrical or plane ones for simplicity$'$s sake. We have not met any rigorous analog solution relative to our representation here except the cases when the quasi-optic approximations may be used as in the fiber optics analysis.

Therefore, we are solving a problem about the effect of normal wave conversion due to an abrupt discontinuity of the transverse electric properties of a terrestrial waveguide in the following model. The ideal spherical model of the Earth with homogeneous electric properties and with its radius R = 6370 km is surrounded by two segments of isotropic ionosphere each of which is determined by its profile of electron concentration $N_e^{I,II}(r)$ and a mutual profile of electron collision frequency with neutrals $\nu_{eff}(r)$. These profiles determine the profiles of electric conductivity $\sigma^I(r)$ or $\sigma^I I(r)$ for the VLF wave propagation. The first inner cone segment containing on its axis a source of the normal radio waves (a transmitter) is a frustum (truncated cone) bounded at its bottom by ground with the impedance boundary conditions for it. The frustum is characterized by a value of angle θ_{irr} in the spherical coordinate system r, θ, φ (with its beginning in the center of Earth), and by a distance from a ground based source to the boundary along the ground surface which is equal to Rθ_{irr}. The second space section is the space characterized by $\theta > \theta_{irr}$.

Our purpose is to determine the reflection coefficient and conversion coefficients for a given normal wave penetrating through the boundary of abrupt medium changing at $\theta = \theta_{irr}$. The inner cone is characterized by undisturbed ionosphere of middle latitudes, and the outer sector is characterized by the ionosphere disturbed by an URE precipitation.

The waveguide properties are determined by a profile of electric conductivity which is increasing exponentially at radial infinity: $\sigma(x) = Im(\varepsilon'(x))\omega$,

$k = \omega\sqrt{\varepsilon'\mu_0} = \omega\sqrt{\varepsilon_m^{'}\varepsilon_0\mu_0} = k_0\sqrt{\varepsilon_m^{'}}$,

$\varepsilon_m^{'}(x) = 1 - \frac{X(x)}{1+jZ(x)}$, $X(x) = \frac{\omega_p^2(x)}{\omega^2}$, $Z(x) = \frac{\nu_{eff}(x)}{\omega}$, where $j = \sqrt{-1}$, $\omega_p(x)$ - the plasma frequency, $x = k_0 r$ is the dimensionless radial coordinate; r – radial coordinate in the spherical coordinate system with the center in the Earth′s center and the polar axis passing through a VLF transmitter (in the United Kingdom, GBR-station in Rugby); R – is the Earth′s radius; k_0 is a wave number for free space; $\varepsilon' = \varepsilon_m' \cdot \varepsilon_0$. The electric conductivity is approximated by two exponential functions for which its logarithm is a function with an ″elbow″ at the altitude $z_0 = r_0 -$R, (*Beloglazov and Zabavina*(1982a), Beloglazov and Zabavina(1982a); *Beloglazov and Zabavina*(1982b), Beloglazov and Zabavina(1982b)). This approximation corresponds to the auroral undisturbed or moderately disturbed low ionosphere, Figure 1 with the curve 1 for $\sigma^I(z)$, where z is an altitude. At a certain distance from the transmitter (S_2 – D, km) a new profile of effective electric conductivity which makes a model of sporadic D_s-layer (for a certain time of disturbance) with the help of significantly other elbow function: either $\sigma_{str}^{II}(z)$ – curve 2 or $\sigma_{pow}^{II}(z)$ – curve 3 (*Bondarenko and Remenets*(2001), Bondarenko and Remenets(2001)), see Figure 1. Due to the pointed models of conductivity profiles the normal waves exist and penetrate until altitude z_2 at which the impedance boundary conditions are used. Therefore, we come to a problem of mode conversion at a transverse boundary of two spherical jointed waveguides with equal width z_2 and sufficiently accurate impedance boundary conditions at the bottom and top waveguide boundaries.

This statement of the simulation problem may seem to be fare away from the real situation because: i) in reality there is a second axis of symmetry connected with the geomagnetic field, which determines a circular zone of very energetic solar proton (100 MeV) (*Dmitriev et al.*(2010), Dmitriev et al.(2010)) and URE precipitations (*Remenets and Astafiev*(2015), Remenets and Astafiev(2015)). Therefore, a normal wave propagating from England to Kola Peninsula is falling on the boundary of irregularity not normally, see figure 1 in (*Remenets and Astafiev*(2016), Remenets and Astafiev(2016)). ii) The real radius of boundary curvature is centered at the South magnetic pole, the center of model cone boundary is placed in England and its radius on earth has value $R\theta_{irr} \simeq$ 2000 km. The first item we ignore because our purpose is to get an estimate of the effect. The second item is insignificant for the problem because the propagation of the electromagnetic waves is characterized by a local principle, which is formulated with the help of the Fresnels zones which are plotted on the base of the transmitter and receiver points in space which are the focuses of the ellipses enveloping the points. The width of a zone is about square root of a product $S_2\lambda \simeq 200$ km, where the first multiplier is the distance between the source in England and the receiver on the Kola Peninsula, and λ is a wavelength for 16 kHz.

New computational problem is as follows. In the first cone section of the spherical model a TM_0 normal wave with a given complex amplitude propagates from the transmitter to the waveguide joint which is described above. It is necessary to find the complex amplitudes of the wave TM_0 penetrated, the complex amplitudes of other normal waves in the second cone section propagating from the junction boundary and the amplitudes of normal waves generated at the boundary of two mediums and propagating to the transmitter. In order to calculate them it is necessary to demand the continuity of complex E_r and H_φ components at the cone boundary. The radial parts of normal waves of a fixed cone section are orthogonal to each other in the complex Hilbert space and this property is sufficient for answering the main question of the investigation: is it necessary to take into consideration the conversion of the normal waves when one determines the southern boundary of URE precipitation?

3 Components of electromagnetic waves in the inhomogeneous electrically conducting medium with the central symmetry

The complex amplitudes $\overrightarrow{E}$ and $\overrightarrow{H}$ of the electromagnetic field in the inhomogeneous electrically conducting medium with the central symmetry satisfy the Maxwell′s equations for the time dependence of a source signal and the fields excepted in the form $exp(-j\omega t)$:

$$rot\overrightarrow{E} = j\omega\mu_0\overrightarrow{H},$$

(1)

$$rot\overrightarrow{H} = -j\omega\varepsilon^{'}\overrightarrow{E},$$

(2)

where $\varepsilon^{'}(r) = \varepsilon(r) + j(\frac{\sigma(r)}{\omega})$.

The fields $\overrightarrow{E}$ and $\overrightarrow{H}$ are expressed due to Hertz vector $\overrightarrow{\Pi}$:

$$\overrightarrow{H} = -j\omega rot\overrightarrow{\Pi},$$

(3)

$$\overrightarrow{E} = \frac{1}{\varepsilon^{'}}rot(rot\overrightarrow{\Pi}),$$

(4)

if the vector $\overrightarrow{\Pi}$ satisfies to the equation

$$rot\{\frac{1}{\varepsilon^{'}}rot(rot\overrightarrow{\Pi})\} - \omega^2\mu_0 rot\overrightarrow{\Pi} = 0,$$

(5)

which may be transformed to the following:

$$rot(rot\overrightarrow{\Pi}) - k^2\overrightarrow{\Pi} - k^2\Phi = 0$$

(6),

where $k(r) = \omega\epsilon'(r)\mu_0 = k_0\varepsilon'_m(r)$; $\varepsilon'_m(r) = \varepsilon'(r)/\varepsilon_0$, and Φ is an any smooth function. The magnitude $\varepsilon'_m(r)$ is characterized here by the central symmetry. In this case the Herz vector has only one component Π_r which satisfies to the following equation

$$\frac{1}{r^2\sin\theta}[\frac{d}{d\theta}(\sin\theta\frac{d\Pi_r}{d\theta})] + \varepsilon^{'}_m\frac{d}{dr}(\frac{1}{\varepsilon^{'}_m}\frac{d\Pi_r}{dr}) + \varepsilon^{'}_m k_0^2\Pi_r = 0,$$

(7)

and the transverse components of the electromagnetic field are expressed by the following relations:

$$H_\varphi = \frac{j\omega}{r}\frac{d\Pi_r}{d\theta},$$

(8)

$$E_r = \frac{1}{\varepsilon'}(\varepsilon_m^{'}\frac{d}{dr}(\frac{1}{\varepsilon_m^{'}}\frac{d\Pi_r}{dr}) + \varepsilon_m^{'}k_0^2\Pi_r).$$

(9)

Correspondingly, the component E_r is expressed with the help of the H_φ component:

$$E_r = \frac{i}{\varepsilon' r\omega\sin\theta}\cdot\frac{\partial(\sin\theta\cdot H_\varphi)}{\partial\theta}.$$

(10)

According to the Maxwell equations (1) and (2) the equation for the H_φ component is gotten:

$$rot[\frac{1}{\varepsilon'}rotH_\varphi] = k_0^2\varepsilon_m^{'}H_\varphi$$

, (11)

that is,

$$\frac{1}{r^2}\cdot\frac{d}{d\theta}(\frac{1}{\sin\theta}\cdot\frac{d(\sin\theta\cdot H_\varphi)}{d\theta}) + \frac{\varepsilon_m^{'}}{r}\frac{d}{dr}(\frac{1}{\varepsilon_m^{'}}\frac{d(r\cdot H_\varphi)}{dr}) + \varepsilon_m^{'}k_0^2H_\varphi = 0.$$

(12)

The equation (7) may be represented as a sum of the angular and radial differential operations relative to the $\Pi_{r,\theta}$: $L_\theta\Pi_r + L_r\Pi_r = 0$, where

$$L_\theta = \frac{1}{\sin\theta}[\frac{d}{d\theta}(\sin\theta\frac{d}{d\theta})],$$

(13)

$$L_r = r^2\varepsilon_m^{'}\frac{d}{dr}(\frac{1}{\varepsilon_m^{'}}\frac{d}{dr}) + r^2\varepsilon_m^{'}k_0^2.$$

(14)

The eigenvalues λ_n of the radial operator L_r , which is defined on the set of functions, which attenuate in the conducting plasma medium against the altitude and satisfy to the impedance boundary conditions on the ground surface, are defined by the followimg equality:

$$L_r\Pi_r = \lambda_n\Pi_r,$$

and as it is $\Pi_r(r,\theta) = U(r)\cdot P(\theta)$ then:

$$L_rU(r) = \lambda_nU(r).$$

(15)

The last equation is transformed into the differential Ricatty equation (17) of first degree if to introduce the impedance function:

$$u(r) = \frac{\frac{dU(r)}{dr}}{\varepsilon_m^{'}(r)\cdot U(r)}.$$

(16)

Then

$$\frac{du(r)}{dr} + \varepsilon_m^{'}(r)\cdot u(r)^2 = -k_0^2 + \frac{\lambda}{\varepsilon_m^{'}(r)\cdot r^2}.$$

(17)

An eigenvalue λ_n is connected with the index of cylindrical functions in the cases of homogeneous medium with $\varepsilon_m = 1$ by the following relation: $\lambda_n = \nu_n^2 - 1/4$. The same parameter ν_n defines the asymptotic angular dependence of the field as follows: $P(\theta) \sim \exp(j\nu_n\theta))$.

Inclusion of the computer integration of this Ricatty equation (17) from a top waveguide boundary to the ground (for which the impedance boundary conditions are given to us) into an iteration process relatively to the ν produces an eigenvalue ν_n and corresponding eigenfunction $U(r, \nu_n)$ according to the (15). According to the (9) the following relation has place for an eigenfunction with number n:

$$E_{r,n} = \frac{1}{\varepsilon_m'(r) \cdot r^2} L_r \Pi_n(r,\theta) \simeq \frac{1}{\varepsilon_m'(r) \cdot r^2} \nu_n^2 \Pi_n(r,\theta) = \frac{1}{\varepsilon_m'(r) \cdot r^2} \nu_n^2 U_n(r) P_n(\theta).$$

(18)

According to the same relation (17) and to the asymptotic relation $P_n(\theta) \sim \exp(j\nu_n\theta)$ one gets the value of the singular magnetic component of the TM_n normal wave with number n:

$$H_{\varphi,n} = \frac{j\omega}{r} \cdot \frac{d\Pi_{r,n}(r,\theta)}{d\theta} = \frac{j\omega}{r} \cdot U_n(r) \cdot \frac{dP_n(\theta)}{d\theta} = -\nu_n \frac{\omega}{r} \cdot U_n(r) \cdot P_n(\theta).$$

(19)

4 The system of equations generated by the demand of continuity of the transverse components of the TM electromagnetic field on the cone boundary of two mediums with different radial properties

According to the electromagnetic law the transverse components E_r (18) and H_φ (19) must be continuous on the boundary surface of two different mediums, that is on the truncated cone with $\theta_{irr} = (S_2 - D)/R$ in our case. In the following we shall consider the conversion of one normal wave, n= 1, into other ones. This normal wave (which according to maknovryb93 is TM_0 normal wave) with a given amplitude is propagating from the cone with index I into to the outer medium with index II. The radial function $U_1(r)$ of its complex amplitude E_r is normalized to value 1 on spherical ground surface boundary ($x = k_0 R$, R is the radius of Earth) inside the cone. In this cone the electromagnetic field is the sum of the falling wave (E_1, H_1), reflected wave ($\mathrm{R}_1 E_{-1}$, $\mathrm{R}_1 H_{-1}$) and the sums of excited normal waves with numbers $n > 1$: $\sum_2^M \mathrm{R}_n E_{-n}$, $\sum_2^M \mathrm{R}_n H_{-n}$. Then

$E_I = E_1 + \sum_{n=2}^M \mathrm{R}_n E_{-n}, \quad H_I = H_1 + \sum_{n=2}^M \mathrm{R}_n H_{-n}.$ (20)

In the outer medium with number (II) the field is the sum of the excited normal waves which are propagating from the boundary:

$E_{II} = \sum_{n=1}^M \mathrm{T}_n E_n, \quad H_{II} = \sum_{n=1}^M \mathrm{T}_n H_n,$ (21)

where the component indexes r and φ are omitted, and T_n are the complex amplitudes of the passed wave with number $n = 1$ and the excited ones. Demanding the continuity of the full field components on the transverse boundary and taking into consideration that ν_n for a wave propagating in positive direction differs from the wave propagating in opposite direction by a sign ($\nu_{-n} = -\nu_n$) we have the following relations for the radial eigenfunctions and the conversion coefficients on the cone boundary:

$\frac{{\nu_1^I}^2}{\varepsilon_{m,I}(x)} U_1^I(x) + \sum_{n=1}^M \mathrm{R}_n \frac{{\nu_n^I}^2}{\varepsilon_{m,I}(x)} U_n^I(x) = \sum_{n=1}^M \mathrm{T}_n \frac{{\nu_n^{II}}^2}{\varepsilon_{m,II}(x)} U_n^{II}(x),$ (22)

$\nu_1^I \cdot U_1^I(x) - \sum_{n=1}^M \nu_n^I \cdot \mathrm{R}_n U_n^I(x) = \sum_{n=1}^M \nu_n^{II} \cdot \mathrm{T}_n U_n^{II}(x),$ (23)

where the integer M is used instead of infinite value. For a value choice $M = 3$ the equality (23) for full H_φ component and the equality (22) for full E_r component may be rewritten in the form (24) and (25) correspondingly:

$$\nu_1^I \left[U_1^I(x) - R_1\, U_1^I(x) - \frac{\nu_2^I}{\nu_1^I}\, R_2\, U_2^I(x) - \frac{\nu_3^I}{\nu_1^I}\, R_3\, U_3^I(x)\right]$$
$$= \nu_1^{II} \left[T_1\, U_1^{II}(x) + \frac{\nu_2^{II}}{\nu_1^{II}}\, T_2\, U_2^{II}(x) + \frac{\nu_3^{II}}{\nu_1^{II}}\, T_3\, U_3^{II}(x)\right],$$

(24)

$$\frac{1}{\varepsilon_m^I(x)} \left[(\nu_1^I)^2\, U_1^I(x) + R_1\, (\nu_1^I)^2\, U_1^I(x) + \right.$$
$$\left. + R_2\, (\nu_2^I)^2\, U_2^I(x) + R_3\, (\nu_3^I)^2\, U_3^I(x)\right] =$$
$$= \frac{1}{\varepsilon_m^{II}(x)} \left[T_1\, (\nu_1^{II})^2\, U_1^{II}(x) + \right.$$
$$\left. + T_2\, (\nu_2^{II})^2\, U_2^{II}(x) + T_3\, (\nu_3^{II})^2\, U_3^{II}(x)\right].$$

(25)

5 Determination of the mode conversion coefficients

By multiplying consequently these last equalities by the eigenfunctions of the not self-adjoint operator of conjugate boundary problem for 2-nd section and by calculating the scalar products according their definition for a not self-adjoint operator (*Titchmarsh*(1946), Titchmarsh(1946); *Keldysh* (1951), Keldysh (1951); *Wait*(1964), Wait(1964); ?, ?; *Makarov and Novikov*(1968), Makarov and Novikov(1968); *Krasnushkin and Baibulatov*(1968), Krasnushkin and Baibulatov(1968); *Krasnushkin*(1969), Krasnushkin(1969); *Pappert and Smith*(1972), Pappert and Smith(1972)) $< U_n * U_m > \equiv \int_{x=k_0R}^{x=k_0(R+z_2)} U_n(x) U_m(x) dx$, which is not equal to zero for $n = m$, one gets the following 6 algebraic relations corresponding to 3 normal waves, used in our numerical calculations, $n = 1, 2, 3$:

$$\nu_1^I\ < U_1^I(x) * U_i^{II}(x) > -$$
$$-R_1\, \nu_1^I\ < U_1^I(x) * U_i^{II}(x) > -$$
$$-R_2\, \nu_2^I\ < U_2^I(x) * U_i^{II}(x) > -$$
$$-R_3\, \nu_3^I\ < U_3^I(x) * U_i^{II}(x) > =$$
$$= T_i\, \nu_i^{II}\ < U_i^{II}(x) * U_i^{II}(x) > \equiv T_i\, \nu_i^{II}\, N_i^{II},$$

(26)

$$(\nu_1^I)^2\ < \frac{\varepsilon_m^{II}(x)}{\varepsilon_m^I(x)}\, U_1^I(x) * U_i^{II}(x) > +$$
$$+R_1\, (\nu_1^I)^2\ < \frac{\varepsilon_m^{II}(x)}{\varepsilon_m^I(x)}\, U_1^I(x) * U_i^{II}(x) > +$$
$$+R_2\, (\nu_2^I)^2\ < \frac{\varepsilon_m^{II}(x)}{\varepsilon_m^I(x)}\, U_2^I(x) * U_i^{II}(x) > +$$
$$+R_3\, (\nu_3^I)^2\ < \frac{\varepsilon_m^{II}(x)}{\varepsilon_m^I(x)}\, U_3^I(x) * U_i^{II}(x) > =$$
$$= T_i\, (\nu_i^{II})^2\ < U_i^{II}(x) * U_i^{II}(x) > = T_i\, (\nu_i^{II})^2\, N_i^{II},$$

(27)

where i is a number of the $U_i^{II}(x)$ eigenfunction used for multiplication, and the N_i^{II} is its norm. We used the following normalization: $U_i^{I,II}(r = R) = 1$.

According to these 6 equation 3 reflection coefficients R_n^I and 3 transition coefficients T_n^{II} were determined for abrupt transition in the waveguide from $\varepsilon_m^I(x)$ to $\varepsilon_m^{II}(x)$, for which σ^I, (σ_{str}^{II}) and (σ_{pow}^{II}) of Figure 1 correspond. They are represented for Table 3.

The data of the lust column (the powerful disturbance (PwD)) of this table were used for getting the relative comparison of the altitude distributions of the terms of the sum at (24), and this comparison is represented for Figure 2. This comparison is approximately correct due to the fact that in our frequency case the first eigenvalues ν_n differ from each other at 4-th – 3-d digits. Therefore, the Figure 2 gives the relative comparison of the complex altitude amplitude of the TM_0 normal wave falling on the $''$ volume$''$ inhomogeneity, caused by an URE precipitation,

(i) with the amplitudes of the TM_0 transmitted $T_1U_1^{II}$ and reflected $R_1U_1^I$,

(ii) with the TM_1 generated by the boundary of inhomogeneity with one of its $T_2U_2^{II}$ part propagating to a receiver and the other $R_2U_2^I$ one of it propagating to the VLF source and

(iii) with the TM_2 normal wave generated by the inhomogeneity with its $T_3U_3^{II}$ part propagating to a receiver and the other $R_3U_3^I$ one of it propagating to the VLF source.

The Table 3 and Figure 2 demonstrate that the conversion effect of TM_0 normal wave into the TM_2 normal wave (with number $n = 3$) is negligible relative to the errors of measurements, and, consequently, our analysis usage of only 3 normal waves is justified.

Therefore, according to the calculations represented we see that at the maximum of a powerful VLF disturbance an effect of main normal wave TM_0 transition $(T_1 \cdot U_1^{II}(z))$ for its amplitude **on ground** (z = 0) is $\approx 15\%$ and for its phase is ≈ 0.2 *rad.* The last value at 3 times greater then the phase measurement error in our case ($1\mu s \sim 0.06$ *rad.* for our working frequency 16 kHz). At the same time we see (Table 3) that for a strong VLF disturbance the calculated result for the main TM_0 normal wave indicates on amplitude decrees at 0.93 times for the maximum and the phase change at 1.2 μs, id est., at 0.07 *rad.* These changes of complex magnitude T_1 are comparable with the measurement errors of the experimental data used by us remast15. More than that, as the determined boundary of URE precipitations is an analysis product of a full disturbance (which is a function of time), then the mode conversion effect for the maximum of a disturbance cannot be extrapolated for all stages of the disturbance. More than that, in the pointed work we used only strong and moderate disturbances (StD and MdD)

It seems that another normal wave TM_1 with $T_2 \cdot U_2^{II}(x)$ ought to be considered in analysis, but it is not so. The difference between the image parts of the eigenvalues for first two normal waves in the disturbed section is so great that the second one which is excited by the first normal wave TM_0 at the inhomogeneity boundary does not achieve a receiver due the greater attenuation.

In addition to the pointed items one ought to consider that in reality there is non abrupt change of the boundary properties. In reality a relatively smooth change, with a space scale about 1 degree changing of electric properties, exists, and, therefore, the represented values of the mode conversion are the above estimations for the real ones.

We state

(i) that existence of a sporadic D_s- layer of electric conductivity appearing under the regular ionosphere D-layer has an electromagnetic proof;

(ii) that in our procedure of southern boundary determination *Remenets and Astafiev*(2015) (Remenets and Astafiev(2015)); *Remenets and Astafiev*(2016) (Remenets and Astafiev(2016)) in which only strong and moderate disturbances (StD′s and MdD′s) caused by the URE precipitations were used the effect of normal wave conversion is negligible. In the case of a powerful disturbance it is necessary to be careful in analysis.

At the same time we may state that in the cases of the most powerful proton precipitations (such as on 16 February 1984 and 29 September 1989) for which the effective height fell down to 50 and 45 km correspondently, *Remenets*(1997) (Remenets(1997)), one may expect the analog qualitative results. But they should be quantitatively weaker significantly due to the absence of bremsstrahlung X-rays and the corresponding sporadic D_s-layer of the electric conductivity below the regular D-layer of the ionosphere.

In addition to the above quantitative results important for the effects connecting with the ultraenergetic relativistic electron ($\sim$ 100 MeV) precipitations *Remenets and Astafiev*(2015) (Remenets and Astafiev(2015)); *Remenets and Astafiev*(2016) (Remenets and Astafiev(2016)); *Remenets and Astafiev*(2019) (Remenets and Astafiev(2019)) we have demonstrated in present paper an efficiency of our not traditional stating of a problem about mode (normal wave) conversion and obtaining its solution. Such type of problems exists more than 50 years but only now it became possible to get the solution of the problem in natural for spherical Earth model statement in which the space in transverse surface of a waveguide is not divided empirically on the air bottom part and electrically active top part. After such dismemberment the previous authors solved the problem of mode conversion from one air part of waveguide to another air part, and the input into conversion of the upper electrically active and different parts being ignored. We consider that in present work we have passed this point of discussion. We considered a mode transition from one transversely inhomogeneous medium to another transversely inhomogeneous medium with the corresponding quantitative results. We consider that our suggested and used approach to the mode conversion will be useful in the waveguides with natural or artificial transverse inhomogeneity the size of which is comparable with the height of a waveguide. Such situation appears not only in the cases of ultraenergetic relativistic electron precipitations coming from the Sun but in the astrophysics cases too *Tanaka et al.*(2008) (Tanaka et al.(2008)), *Tanaka et al.*(2010) (Tanaka et al.(2010)). Very short (much less than one second) hard γ ray bursts from a certain space point illuminate the half of Earths atmosphere, create the corresponding D_s layer of electric conductivity in the middle and low atmosphere. The problem of transverse $''$ volume$''$ inhomogeneity boundary appears too.

Relative success of our analysis is due to the fact that the spectra of radial (transvers) not self-adjoint operator for the problem of electromagnetic wave diffraction at a sphere is discrete (*Fock*(1965), Fock(1965)). How to solve analytically a problem of reflection of plain wave from an electrically inhomogeneous in one transverse dimension plane we dont know.

Again we have right to remind that the ultraenergetic relativistic electrons being the cause of present investigation are the electron-killers with energy $\sim$ 100 MeV which ought to be much more dangerous than the traditional relativistic ones with energy $\sim$ 1 - - 10 Mev.

Acknowledgments

As we explained in the Introduction, the present investigation is based on our previous solutions of inverse VLF problem (*Remenets and Beloglazov*(1999), Remenets and Beloglazov(1999)), (*Beloglazov and Remenets*(2005), Beloglazov and Remenets(2005)). These solutions are based on the experimental data of the Polar Geophysical Institute, Apatity, Murmansk reg., Russian Federation, which are represented for figure 2 of (*Remenets and Beloglazov*(1985), Remenets and Beloglazov(1985)), for table 2 of (*Remenets*(1997), Remenets(1997)), for figures 1 and 2 of (*Remenets and Beloglazov*(1999), Remenets and Beloglazov(1999)), for figures 3 – 4 of (*Remenets and Beloglazov*(1992), Remenets and Beloglazov(1992)), for p. 240-261 of Application 6 to (*Remenets*(2005), Remenets(2005)), for figures 3 – 4 and table 4 for belrem05, for figures 3 – 5 and tables 1 – 2 of (*Remenets and Beloglazov*(2013), Remenets and Beloglazov(2013)), for the figure and tables of (*Remenets and Beloglazov*(2015), Remenets and Beloglazov(2015)), for the tables of (*Remenets and Shishaev*(2019), Remenets and Shishaev(2019)).

References

Andriani, O. (2017), Ten years of PAMELA in Space (Review), *Revista del Nuovo Cimento*, *40*, issue 10, 473-522. DOI: 10.1393/ncr/i2017-10140-x

Bahar E., Wait J. R. (1965), Propagation in a model terrestrial waveguide of nonuniform height: theory and experiment. *Radio Sci.*, 69D, issue 11, 1445-1452.

Beloglazov M. I., and I. N., Zabavina (1982), About an effective model of the quiet auroral ionosphere for VLF. *Geomagnetizm i Aeronomiya*, 22, issue 2, 319-320. (In Russian)

Beloglazov M. I., and I. N., Zabavina (1982), Effective model of the low ionosphere for VLF during auroral disturbances. *Geomagnetizm i Aeronomiya*, 22, issue 3, 492-493. (In Russian)

Beloglazov, M. I., and G. F. Remenets (2005), Investigation of powerful VLF disturbances, *Intern. J. Geom. Aeronomy*, 5, issue 3, April issue, GI3004, https://doi.org/10.1029/2005GI000101

Beloglazov, M. I., G. F., Remenets, and V. P. Nemirov (1998), Upper atmosphere ionization by the REP's in 1985 – 86 and VLF inverse problem. In: *Physics of Auroral Phenomena, Proceedings of the 21st Annual Apatity Seminar.*, edited by. B. V. Kozelov (Polar Geophysical Institute of RAS, Apatity, Russia), 16-18.

Bondarenko, V. V. and G. F. Remenets (2001), Numerical analysis of the ionized atmosphere, *Physics of auroral Phenomena, Proceedings of the 24-th Annual Seminar, Apatity, 27 February – 2 March 2001*, Polar Geophysical Institute – RAS, Apatity, Murmansk reg., p. 103-106.

Callis L. B., D. N. Baker, J. B. Blake, J. D. Lambeth, R. E. Boughner, M. Natarajan, R. W. Klebesadel, and D. J. Gorney, (1991) Precipitating relativistic electrons: their long-term effect on stratospheric odd nitrogen levels, *J. Geophys. Res.*, *96*, No. D2, 2939-2976.

Dmitriev, A.V., Jahachandran, P.T., Tsai, L.-C., 2010, Elliptical model of cutoff boundaries for the solar energetic particles measured by POES satellites in December 2006. *J. Geophys. Res.*, *115*, A12244; doi: 10.1029/2010JA015380.

Fock V. A. (1965), *Electromagnetic Diffraction and Propagation Problems*, (Pergamon Press).

Galeys J., (1964), Propagation of VLF waves below a curved and stratified anisotropic ionosphere, *J. Geophys. Res.*, *69*, issue 17, 3639-3650.

Galeys J. (1968), Propagation of ELF and VLF waves below an anisotropic ionosphere with a dipping static magnetic field, *J. Geophys. Res.*, *73*, issue 1, 339-352.

Galeys J. (1969), VLF modes below an idealized anisotropic ionosphere, *Radio Science*, *4*, issue 6, 491-516.

Galyuk, U. P., and V. I. Ivanov (1978), Determination of VLF characteristics for Earth-ionosphere waveguide with vertical anisotropic inhomogeneity, In: *Problems of Diffraction and Wave Propagation*, issue 16, 148-154. Leningrad State University, St. Petersburg (In Russian).

Gyunninen, E. M., and I. N. Zabavina, (1966), Propagation of long waves above the Earth surface. In:*Problems of Diffraction and Wave Propagation*, issue 5, 3-30. Leningrad State University, Leningrad, USSR. (in Russian).

Keldish, M. V. (1951), On the characteristic va1ues and characteristic functions of certain classes of not-selfadjoint equations, *Dokl. Academ. Nauk*, *77*, 11-14. Moscow, USSR.

Krasnushkin, P. E., and R. B. Baibulatov, (1968), Calculation of wave numbers of normal waves in a spherically stratified media by the method of recalculation of the impedance, *Reports of the USSR ACADEMY OF SCIENCES*, *182*, 294-297, Moscow.

Krasnushkin P. E., (1969) Decomposition at normal waves in a spherically stratified medium, *Reports of the USSR ACADEMY OF SCIENCES*, *185*(6), 1262-1265, Moscow.

Makarov, G.I., and V. V., Novikov (1968), Radio wave propagation in the impedance plane and spherical waveguides. In: *The problems of wave diffraction and propagation*, Issue 7, 19-33. (In Russion).

Makarov, G. I., V. V., Novikov, and S. T., Rybachek (1993), *Radio wave Propagation in the Earth-ionosphere Waveguide and in the Ionosphere*, "Nauka", Moscow, 152 p. (In Russian).

Osadchy, A. P. and G. F. Remenets (1979), Some features of VLF mode conversion in the Earth-anisotropic ionosphere waveguide, *Problems of the Wave Diffraction and Propagation*, issue 17, 141-147.

Pappert, R. A., and J. A. Ferguson (1986), VLF/LF mode conversion for air-to-air transmission in the Earth-ionosphere waveguide, *Radio Science 21*, p. 551.

Pappert, R. A., and D. G. Morfitt (1972), Some results of a mode-conversion program for VLF, *Radio Science 7*, issue 10, p. 913-923.

Pappert, R. A., and R. R. Smith (1972), Orthogonality of VLF height gains in the earth ionosphere waveguide, *Radio Science 7*, issue 2, 275-278.

Pesnell, W. D., R. A. Goldberg, C. H. Jackman, D. L. Chenette, and E. E. Gaines (1999), A search of UARS data for ozone depletions caused by the highly relativistic electron precipitation events of May 1992, *J. Geophys. Res., A1, 104*, 165-175.

Remenets, G. F. (1994), Unmonotony of electron concentration profile of the low auroral ionosphere in the case of relativistic electron precipitation on 15 September 1982, *The Problems of the Wave Diffraction and Propagation*, issue 26, p. 35-42. (In Russion)

Remenets, G. F. (1997), Unique ground VLF monitoring of the relativistic electron precipitations. In: *Problems of Geospace. Proceedings of an International Conference "Problems of Geocosmos" held in Petrodvorets, St.Petersburg, Russia*, Ed.: M. I. Pudovkin, B. P. Besser, W. Riedler, and A. M. Lyatskaya (Austrian Acad. Sci. Press, Vienna), pp. 273-278.

Remenets, G. F. (2005), Studying the dynamics of electric properties of the middle and lower ionosphere based on interference data of ultralow-frequency radio waves, Doctoral (Phys. - - Math.) Dissertation, St. Petersburg State University, St. Petersburg, 261 p.

Remenets, G. F., and A. M. Astafiev (2015), Southern boundaries of ultra-energetic relativistic electron precipitations in several cases from 1985 1986 years, *J. Geophys. Res. – Space Physics*, 120, issue 5, 3318-3327. http://doi.org/10.1002/2014JA020591

Remenets, G. F., and A. M., Astafiev (2016), Solution uniquity of an inverse VLF problem: A case-study of the polar, ground-based, VLF radio signal disturbances caused by the ultra-energetic relativistic electron precipitations and of their southern boundaries, *Advances in Space Research*, 58, 878-889. https://doi.org /10.1016/j/asr.2016.05.45.

Remenets G. F., and A. M. Astafiev, (2019), Generalized Schumann and variation moment methods used for the determination of the equatorward boundary of the ultra-energetic relativistic electron precipitations into the auroral middle atmosphere *J. Atmospherical and Solar-Terrestrial Physics*, *182*, 186-193; https://doi.org/10.1016/j.jastp.2018.11.019

Remenets, G. F., and M. I. Beloglazov (1985), Reflection properties of the low polar ionosphere, the peculiarities of intoxication and propagation of the VLF waves at high latitudes, *Izvestiya Vuzov. Radiofysika, 28*, 1491-1504, (It was translated in English by Springer Editor: *Radiophys. Quantum Electron.*, *28*(12), 1029-1040. DOI: 10.107/BF01034159)

Remenets, G. F., and M. I. Beloglazov, (1992), Dynamics of an auroral low ionospheric fringe at geophysical disturbances on 29 September 1989, *Planet Space Sci.*, *40*, 1101-1108.
Remenets, G. F., and M. I. Beloglazov, (1999) Ground VLF monitoring of the ultra-relativistic electron precipitations, in *Problems of Geospace 2, Proceedings of the 2nd International Workshop held in Petrodvorets, St.Petersburg, Russia*, edited by V. S. Semenov, H. K. Biernat, M. V. Kubyshkina, C. J. Farrugia, and S. Mühlbachler, (Austrian Acad. Sci. Press, Vienna), 275-281.
Remenets, G. F., and M. I. Beloglazov, (2013), Ultrarelativistic electrons in the near cosmos and X-ray aurora in the middle polar atmosphere, *JGR - Space Physics*, *118*, issue 11, 6829-6838. DOI: 10.1002/2013JA018822.
Remenets, G. F., and M. I. Beloglazov, (2015), Geomagnetic cutoff effect as an evidence for the corpuscular nature of anomalous VLF disturbances, *Geomagnetism and Aeronomy*, *55*, 1, pp. 98-107. Original Russian text was published in Geomagnetizm i Aeronomiya, *55*(1), 103-112. DOI: 10.1134/S0016793214060152
Remenets, G. F., and V. A. Shishaev, (2015), VLF wave propagation and middle polar atmosphere as a detector of ultra-energetic relativistic electron precipitations in 1988 1992, *JASTP*, *196*, December 2019, 105145. DOI: 10.1016/j.jastp.2019.105145
Satio Hayakawa (1969), *Cosmic Ray Physics*, edited by John Wiley and Sons (N. Y., London, Sydney, Toronto).
Smith R. (1977), Mode conversion coefficients in the Earth-ionosphere waveguide for VLF propagation below a horizontally stratified anisotropic ionosphere, *J. Atm. and Solar – Terr. Phys.*, *39*(4), 510-517.
Tanaka, Y. T., T. Terasawa, M. Yashida, et al., (2008), Ionospheric disturbances caused by SGR 199 + 14 giant gamma ray flare in 1998: Constraints on the energy spectrum of the flare, *J. Geophys. Res.*, *113*, A07307. doi: 10.1029/2008Ja 013119
Tanaka, Y. T., J. P. Raulin, F. C. P. Bertony, et al., (2010), First very low frequency detection of short repeated bursts from magnetar SDR J1550-5418, *Astrophys. J. Letters*, *721*, L24-L27. doi: 10.1088/2041-8205/721/1/L24
Titchmarsh, E. C. (1946), *Eigenfunction Expansions Associated with Second-order Differential Equations*, at the Clarendon Press, Oxford.
Wait, J. R., (1964), Two-dimensional treatment of mode theory of the propagation of VLF radio waves, *Radio Science*, *68D*(1), 81-93.
Wait, J. R., (1968), On the theory of VLF propagation for a step model of the nonuniform Earth-ionosphere waveguide, *Canad. J. Phys, 17*, 1979-1983. DOI: 10.1139/p68-539
Wait, J. R., Spies, K. P. (1968), On the calculation of mode conversion at a graded height change in the earth-ionosphere waveguide at VLF. *Radio Sci.*, *3*, 787-791.

Table 1. **Results of the inverse VLF problem solutions** for three UT moments for URE precipitation on 29 September 1989 gotten by using the normal wave theory of propagation. The computed values are given in brackets for comparison with the experimental ones. [a]

Time moment of the disturbance, UT	0600	0730	0900
$\frac{(A_1)_d}{(A_1)_c}$	0.7 ± 0.1 (0.9)	0.5 ± 0.1 (0.6)	0.7 ± 0.1 (0.9)
$\varphi_{1c} - \varphi_{1d}$, μs	3.6 ± 0.5 (4.3)	8.6 ± 1.5 (8.1)	5.2 ± 0.5 (5.0)
$\frac{(A_2)_d}{(A_2)_c}$	0.7 ± 0.1 (1.0)	0.6 ± 0.2 (0.7)	0.7 ± 0.1 (0.8)
$\varphi_{2c} - \varphi_{2d}$, μs	2.0 ± 0.5 (1.7)	0.6 ± 1.5 (7.5)	4.4 ± 0.5 (6.1)
$\frac{(A_3)_d}{(A_3)_c}$	0.6 ± 0.1 (0.7)	0.6 ± 0.1 (0.6)	0.7 ± 0.1 (0.7)
$\varphi_{3c} - \varphi_{3c}$, μs	2.0 ± 0.5 (3.4)	4.5 ± 1.5 (5.6)	4.0 ± 0.5 (3.6)
z_1, km	60 ± 1	58 ± 2	60 ± 1
β, 1/km	-0.01 ± 0.01	-0.04 ± 0.01	-0.02 ± 0.01
h', km	56 ± 1	50 ± 2	54 ± 1
h'', km	55 ± 1	46 ± 2	54 ± 1
h''', km	50 ± 3	43 ± 2	52 ± 2
h, km	57-60	48-49	55-56

[a] The URE precipitation took a place at 0400 – 1000 UT interval. The values $(A_j)_c$ and $(\varphi_j)_c$ were referred to 0400 UT, rembel92.

Table 2. Results of the inverse VLF problem solutions for the UT moments of disturbance maximum for URE precipitation on 21 and 22 January 1992 gotten by using the normal wave theory of propagation, polar night conditions. The computed values are given in the brackets for comparison with the experimental ones.[b]

Date	21 Jan. 1992	21 Jan. 1992	21 Jan. 1992	21 Jan. 1992
Time of disturbance maximum, UT	2250	2250	0740	0740
z_0, km	70	75	70	75
$\frac{(A_1)_d}{(A_1)_c}$	0.04 ± 0.04 (0.09)	0.04 ± 0.04 (0.14)	0.08 ± 0.04 (0.09)	0.08 ± 0.04 (0.15)
$\varphi_{1c} - \varphi_{1d}$, μs	12 ± 1 (15)	12 ± 1 (13)	13 ± 1 (15)	13 ± 1 (13)
$\frac{(A_2)_d}{(A_2)_c}$	0.10 ± 0.03 (0.07)	0.10 ± 0.03 (0.12)	0.09 ± 0.03 (0.07)	0.09 ± 0.03 (0.13)
$\varphi_{2c} - \varphi_{2d}$, μs	20 ± 1 (18)	20 ± 1 (19)	18 ± 1 (18)	18 ± 1 (19)
$\frac{(A_3)_d}{(A_3)_c}$	0.17 ± 0.07 (0.07)	0.17 ± 0.07 (0.19)	0.11 ± 0.04 (0.07)	0.11 ± 0.04 (0.20)
$\varphi_{3c} - \varphi_{3d}$, μs	23 ± 1 (21)	23 ± 1 (24)	22 ± 1 (21)	22 ± 1 (23)
z_1, km	66	67	66	68
β, 1/km	-0.09	-0.07	-0.09	-0.07
h', km	30	36	30	37

[b]The values of "knee" altitude z_0 for the electron profile were taken equal to either 70 or 75 km in order to estimate the influence of its uncertainty on the z_1 and β parameters of a sporadic D_s-layer.

Table 3. The values of complex reflection and transition coefficients R_j and T_j for two models of inhomogeneity junction: with the conductivity profiles $\sigma^{II}_{str}(x)$ and $\sigma^{II}_{pow}(x)$, Fig. 1.[c]

Sporadic D_s layer	$\sigma^{II}_{str}(x)$	$\sigma^{II}_{pow}(x)$
R_1	- 0.0005 + j0.0008	- 0.001 + j0.003
T_1	+ 0.9223 + i0.1095	+ 0.839 + j0.188
R_2	+ 0.0010 - j0.0013	+ 0.004 - j0.005
T_2	+ 0.0872 - j0.1216	+ 0.179 - j0.174
R_3	- 0.0004 + j0.0006	- 0.001 + j0.001
T_3	- 0.0168 - j0.0150	- 0.019 - j0.006

[c] The undisturbed conductivity profile was σ^I, Fig. 1.

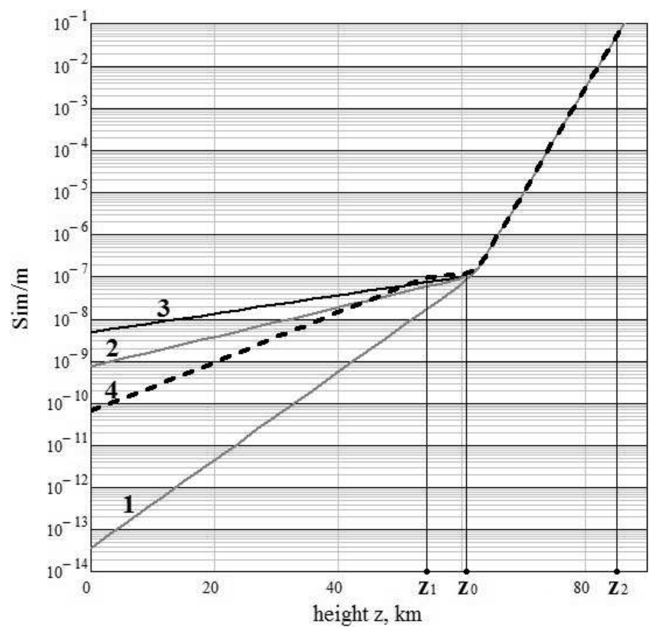

Figure 1. The effective profiles of electric conductivity for undisturbed (σ^I – curve 1) and disturbed (σ^{II}_{str} – curve 2, σ^{II}_{pow} – curve 3) conditions. The bottom indexes of electric conductivity $''str''$ and $''pow''$ correspond to the maximums of a strong and a powerful VLF disturbances bondrem01, belrem05. Undisturbed auroral profile σ^I was taken from the work belzab82a.

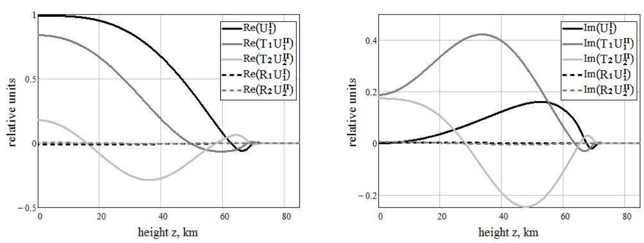

Figure 2. Comparison of the altitude distributions for the complex amplitudes of the converted normal waves in the waveguide by the longitudinal D_s heterogeneity. The source of excitation is a normal wave TM_0 ($U_1^I(x)$ normalized to 1 at $x = k_0R$) propagating to the cone boundary. The left and right parts of the panel are the real and image parts of the magnitudes.

Figure 1.

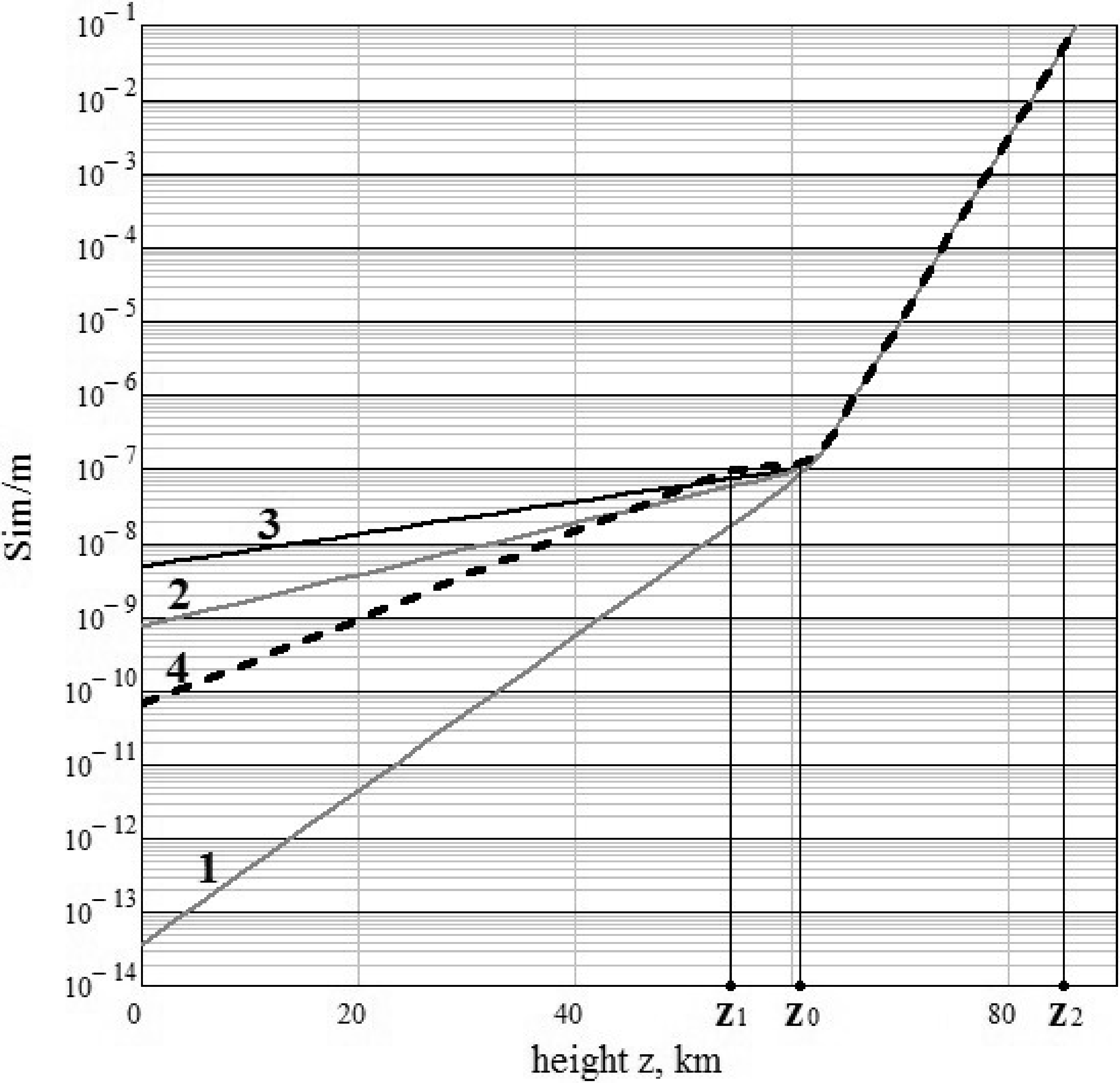

Sim/m
10^{-1}
10^{-2}
10^{-3}
10^{-4}
10^{-5}
10^{-6}
10^{-7}
10^{-8}
10^{-9}
10^{-10}
10^{-11}
10^{-12}
10^{-13}
10^{-14}
3
2
4
1
0
20
40
z_1
z_0
80
z_2
height z, km

Figure 2.

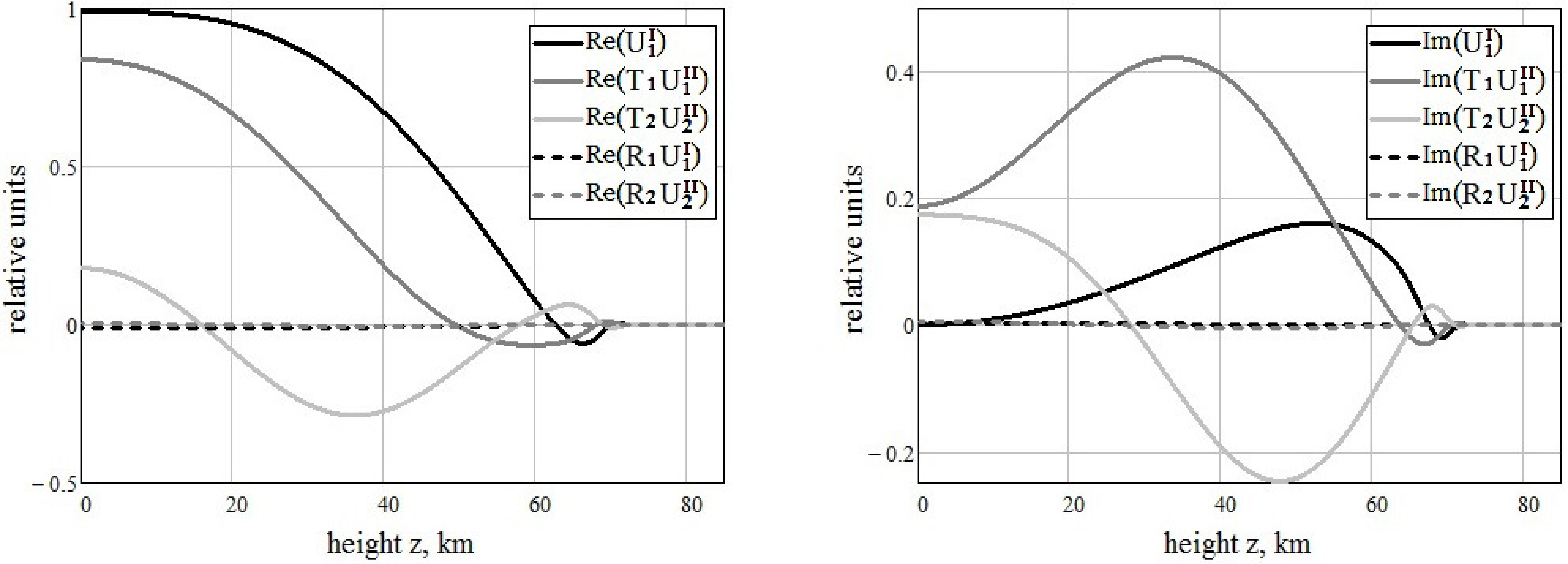

relative units
height z, km
1
0.5
0
−0.5
0
20
40
60
80
Re(U_1^{I})
Re($T_1U_1^{II}$)
Re($T_2U_2^{II}$)
Re($R_1U_1^{I}$)
Re($R_2U_2^{II}$)
relative units
height z, km
0.4
0.2
0
−0.2
0
20
40
60
80
Im(U_1^{I})
Im($T_1U_1^{II}$)
Im($T_2U_2^{II}$)
Im($R_1U_1^{I}$)
Im($R_2U_2^{II}$)